ACS APPLIED MATERIALS & INTERFACES

Research Article

www.acsami.org

Directly Drawn Poly(3-hexylthiophene) Field-Effect Transistors by Electrohydrodynamic Jet Printing: Improving Performance with Surface Modification

Yong Jin Jeong,[†,‡,∥] Hyungdong Lee,[§,∥] Byoung-Sun Lee,[‡] Seonuk Park,[†] Hadi Teguh Yudistira,[§] Chwee-Lin Choong,[‡] Jong-Jin Park,*[,‡] Chan Eon Park,*[,†] and Doyoung Byun*[,§]

[†]POSTECH Organic Electronics Laboratory, Polymer Research Institute, Department of Chemical Engineering, Pohang University of Science and Technology, Pohang 790-784, Korea

[‡]Samsung Advanced Institute of Technology (SAIT), Yongin 449-712, Republic of Korea

[§]Department of Mechanical Engineering, Sungkyunkwan University, Suwon, Gyeonggi 440-746, South Korea

Supporting Information

ABSTRACT: In this study, direct micropatterning lines of poly(3-hexylthiophene) (P3HT) without any polymer binder were prepared by electrohydrodynamic jet printing to form organic field-effect transistors (OFETs). We controlled the dielectric surface by introducing self-assembled monolayers and polymer thin films to investigate the effect of surface modifications on the characteristics of printed P3HT lines and electrical performances of the OFETs. The morphology of the printed P3HT lines depended on the surface energy and type of substrate. The resulting OFETs exhibited high performance on octadecyltrichlorosilane-modified substrates, which was comparable to that of other printed P3HT OFETs. In order to realize the commercialization of the OFETs, we also fabricated a large-area transistor array, including 100 OFETs and low-operating-voltage flexible OFETs.

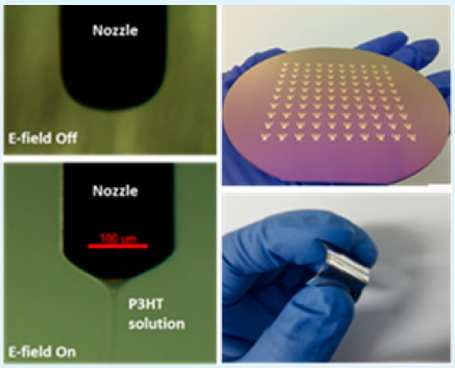

KEYWORDS: *electrohydrodynamic printing, low voltage, flexible device, P3HT, organic field-effect transistors*

INTRODUCTION

Organic field-effect transistors (OFETs) have received considerable attention because of their low-temperature solution processing and various potential applications in low-cost, large-area, and flexible electronics such as display backplanes,[1] radio frequency identification tags,[2] integrated sensors,[3,4] and disposable electronics.[5] A major challenge in commercializing OFETs is the development of inexpensive large-scale fabrication methods. Although many groups have attempted to develop a variety of promising fabrication processes, including roll-to-roll screen printing, doctor blading, and spray printing, these methods need to have additional patterning steps such as masking or etching processes.[6−8] To reduce the fabrication steps, the direct writing technique has been an alternative approach because it integrates the deposition and patterning processes in one step.[9,10]

However, because contact with the substrates damages the surface and hinders the molecular organization of organic materials, degrading electrical performances when making electronic devices, the noncontact direct writing approach is considered to be a promising technique for use in electronic devices.[6] Among established noncontact techniques such as ink or aerosol jet printing,[11−14] electrohydrodynamic (EHD) jet printing, which is also defined as a near-field electrospinning,[15,16] has recently gained much interest as a key method for high-resolution patterning.[17−21] Although other jet printing techniques such as piezoelectric jet printing depend only on a pumping force,[22,23] the electrostatic, hydrostatic, and capillary forces simultaneously operate in EHD jet printing because a strong electric field is applied between the tip of the nozzle and the substrate.[20] The combination of push-and-pull forces elongates the solution and makes continuous jet lines, the widths of which are smaller than the diameter of the nozzle. This unique capacity makes EHD jet printing an attractive technique for large-area and fine patterning at a high resolution. Lee et al. recently established an efficient application of EHD-printed regioregular poly(3-hexylthiophene) (P3HT)/polymer nanowires using an insulating polymer binder for the fabrication of OFETs.[21] However, because charge transport of P3HT is achieved by its crystalline nanofibrillar structures, binder-free P3HT is more favorable for facilitating high electrical mobility and current. Moreover, the dimensions and crystallinity of printed P3HT could be controlled by covering the dielectric surface with various organic materials.[24] Therefore, in-depth studies are needed regarding the influence of the

Received: April 29, 2014
Accepted: June 19, 2014
Published: June 19, 2014

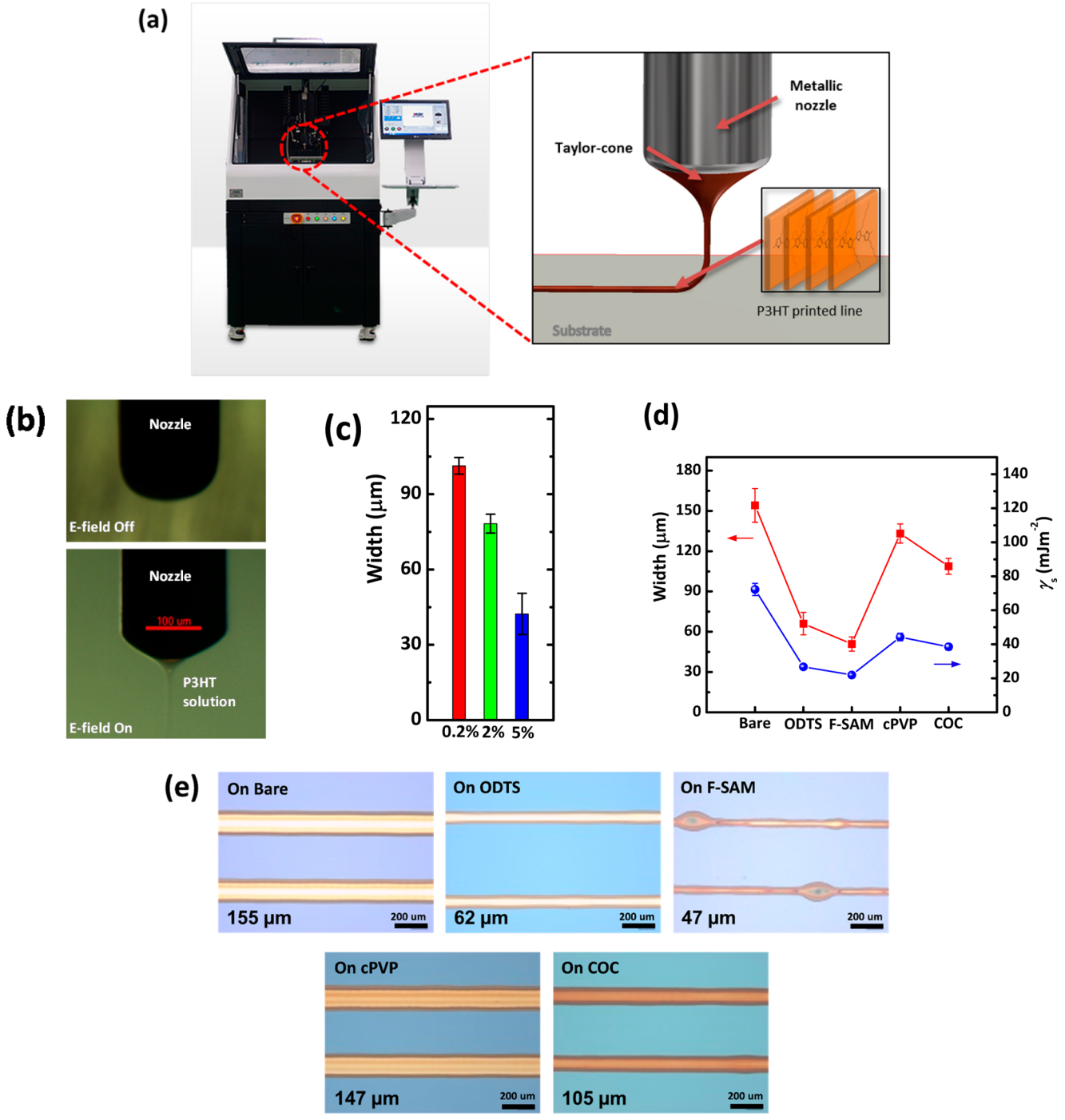

Figure 1. (a) Electrohydrodynamic (EHD) jet printing machine (EnJet Inc., Korea) and near-field EHD jet printed line of P3HT solution from metallic micronozzle. (b) Snapshot images through a CCD camera during the printing process. (c) Line width of printed P3HT according to solution concentration. (d) Comparison of surface energy (γ_s) and line width of P3HT printed onto various types of substrate. (e) Optical microscope images of P3HT lines on each substrate.

dielectric surface on the characteristics of an EHD printed P3HT line.

Here, we prepared microscale line patterning of P3HT without any polymer binder directly onto various substrates using the EHD jet printing technique toward the fabrication of OFETs. For obtaining a stable jet from the nozzle, the concentration of P3HT solution, applied voltage, printing speed, and tip-to-the-collector distance (TCD) were optimized. Moreover, we treated the surfaces of the substrates with a variety of self-assembled monolayers (SAMs) and polymer thin films to investigate the effect of surface modifications on the characteristics of the resolution of printed lines and the electrical performance of the OFETs. As the surface energy decreased and the contact angle values of both water and P3HT solution dropped on the modified surface increased, the width of the printed P3HT line decreased. The OFETs prepared with EHD-printed P3HT on a CH_3-terminated SAM-modified surface exhibited good performances, with a mobility of 0.045 $cm^2/(V\ s)$. Finally, the EHD printing technique of P3HT enabled the fabrication of a large-area OFETs array and low-

dx.doi.org/10.1021/am502595a | ACS Appl. Mater. Interfaces 2014, 6, 10736−10743

operating-voltage flexible devices with good bending stability under 1.5% bending strains.

EXPERIMANTAL METHODS

Materials and Sample Preparation. Highly *n*-doped Si wafers with 300 nm thick thermally grown SiO_2 layers were used as substrates. Regioregular poly(3-alkylthiophenes) (P3HT), anhydrous toluene, 1*H*,1*H*,2*H*,2*H*-perfluorooctyltriethoxysilane (F-SAM), *n*-butylamine, poly(4-vinylphenol) (PVP), poly(melamine-*co*-formaldehyde) methylated (PMF), and *N*,*N*-dimethyl formaldehyde were purchased from Sigma-Aldrich. Octadecyltrichlorosilane (ODTS) was purchased from Gelest, Inc. Ethylene-norborene cyclic olefin copolymer (COC, $T_g \sim 180$ °C) was purchased from Polyscience. All materials were used as received without further purification. The *n*-doped Si/SiO_2 substrates were cleaned in a hot piranha solution followed by multiple rinses with distilled water. Cleaned substrates were exposed to a UV tip cleaner for 20 min for further hydrophilization. For surface modification with self-assembled monolayers (SAMs), the substrates were dipped in ODTS and F-SAM dissolved in toluene for 30 min. In the F-SAM solution, *n*-butylamine was added as a stabilizer. The samples were subsequently baked at 120 °C for 20 min followed by sonication in toluene for 15 min. For surface treatment with polymer thin films, PVP and PMF as a cross-linker dissolved in *N*,*N*-dimethyl formaldehyde and COC dissolved in toluene were spin-coated on the *n*-doped Si/SiO_2 substrates. The PVP films containing PMF were baked at 180 °C for 1 h to induce cross-linking. The COC film was baked at 120 °C for 30 min to remove any residual solvent. To print an organic semiconductor, P3HT solution in toluene was stirred on a hot plate at 70 °C for complete solubilization. The P3HT solution was printed onto a variety of substrates at constant temperature (22.5 °C) and humidity (45%) using the EHD printing machine (Enjet Inc., Korea). To complete the fabrication of OFETs, 50 nm thick Au source and drain (S/D) electrodes were thermally evaporated onto printed P3HT lines to achieve a top-contact configuration.

For the fabrication of flexible and low-operating-voltage OFETs, polyethersulfon (PES) substrates were washed with acetone and distilled water multiple times. An aluminum gate electrode was thermally evaporated on PES substrates, and 50 nm thick Al_2O_3 dielectric layers were then prepared by plasma-enhanced atomic-layer deposition (PEALD) (LTSR-150, Leintech). Trimethylaluminum (TMA, Lake LED materials) was injected into the chamber as an aluminum precursor, and O_2 plasma was used as the oxygen source. The film was grown on the substrate at a constant temperature of 100 °C with 200 W RF plasma power.

Characterization. The surface energies of the five different types of surface-treated SiO_2/Si substrates were evaluated by measuring the contact angles (θ) of two test liquids, namely, water and diiodomethane (SEO300A). The total surface energy (γ_s) was calculated from the sum of the dispersion force component of the surface energy (γ_s^d) and the polar force component of the surface energy (γ_s^p) with the following equation[25]

$$1 + \cos\theta = \frac{2(\gamma_s^d)^{1/2}(\gamma_l^d)^{1/2}}{\gamma_l} + \frac{2(\gamma_s^p)^{1/2}(\gamma_l^p)^{1/2}}{\gamma_l} \quad (1)$$

where γ_l is the surface energy of the test liquid (γ_l of water = 72.2 mJ m^{-2}; γ_l of diiodomethane = 50.8 mJ m^{-2}), γ_l^d is the dispersion force component of the surface energy (γ_l^d of water = 22.0 mJ m^{-2}; γ_l^d of diiodomethane = 48.5 mJ m^{-2}), and γ_l^p is the polar force component of the surface energy (γ_l^p of water = 50.2 mJ m^{-2}; γ_l^p of diiodomethane = 2.3 mJ m^{-2}).

All electrical measurements were performed using Keithley 4200 SCS in an N_2-rich glovebox. The morphology of the printed P3HT lines was investigated using atomic force microscopy (AFM) (Multimode AFM, Digital Instruments) and an optical microscope. P3HT solution viscosity was measured by using rotational viscometer (Brookfield Viscometers Ltd., DV-II+LV viscometer)

RESULTS AND DISCUSSION

As shown in Figure 1a, an EHD jet printing machine (EnJet Inc.) was used in this study. To form a continuous P3HT jet without using a polymer binder, the electric charge was induced at the surface of the meniscus of the P3HT solution by applying the electric field between the metallic nozzle (i.d. = 0.1 mm; o.d.= 0.23 mm) and the substrate at 1.8−2.0 kV and supplying the P3HT solution to the nozzle at a flow rate of 0.5−0.8 μL/min. The distance between nozzle tip and substrate (i.e., the tip-to-collector distance (TCD)) was adjusted at around 1 mm. At a speed of 20−30 mm/min, we achieved a stable printing process and a straight-printed P3HT line. Figure 1b shows captured images of the ejection of the P3HT solution before and after applying the electric field. The conical shape of the P3HT solution, known as a Taylor-cone, was clearly seen when the electric field was applied. This Taylor-cone was formed because the electrostatic force was stronger than the surface tension, and the viscosity of the solution was enough to sustain the electrical stress that stretched the meniscus in the direction of the field.[19]

In order to obtain a fine printed line, we varied the concentration of the P3HT solution to 0.2, 2, and 5 wt % to find the optimum conditions for printing. Figure 1b depicts the width of the P3HT lines according to the three concentrations. To investigate the effects of concentration only, the surface was equally modified by ODTS. As the concentration of the P3HT solution increased, the line width dramatically decreased under the same experimental conditions (voltage (1.85 kV), flow rate (0.5 μL/min), printing speed (25 mm/min), and TCD distance (1 mm)) because of the viscosity effect (pure toluene ≈ 0.58 cP, P3HT solution of 0.18 wt % ≈ 0.66 cP, 1.96 wt % ≈ 1.88 cP, and 3.98 wt % ≈ 5630 cP). However, because toluene is a characteristically volatile solvent, the excessively highly viscous solution (≥5 wt %) easily blocked the nozzle tip. In other words, the high concentration of the P3HT solution was easily solidified near the nozzle tip. In this study, 2 wt % of toluene based P3HT was an outstanding proportion for use in the EHD jet printing as well as for the performance of the OFETs.

To investigate the effects of the surface modification on the morphology of the printed P3HT, we introduced five different types of surface treatments: nontreated (bare), CH_3-terminated SAM (ODTS), F-terminated SAM (F-SAM), PVP with cross-linking (cPVP), and cyclic olefin copolymer (COC) treatment. ODTS and F-SAM were chosen to control the surface energy. Moreover, surface modification with ODTS could be used to achieve the highly crystalline growth of overlaying P3HT, thereby enhancing the OFETs performance because the field-effect mobility is always influenced by the crystalline morphology of the organic semiconductor films.[26] cPVP and COC were selected because they are conventionally used as polymer-modifying layers for electronic devices due to their high thermal stability.[27,28] Figure 1c shows the values of surface energy (γ_s) and the width of the P3HT lines on the five different surfaces. The highest γ_s value was obtained for the bare surface ($\gamma_s \approx 72.2$ mJ m^{-2}), whereas F-SAM was the most hydrophobic surface ($\gamma_s \approx 21.9$ mJ m^{-2}). Under constant experimental conditions, such as voltage (1.85 kV), flow rate (0.5 μL/min), printing speed (25 mm/min), and TCD distance (1 mm), we found that the width of the P3HT lines decreased as the surface energy decreased because of the lower surface wettability of P3HT/toluene on the hydrophobic surface.[29] The smallest line width was obtained on the F-SAM-modified

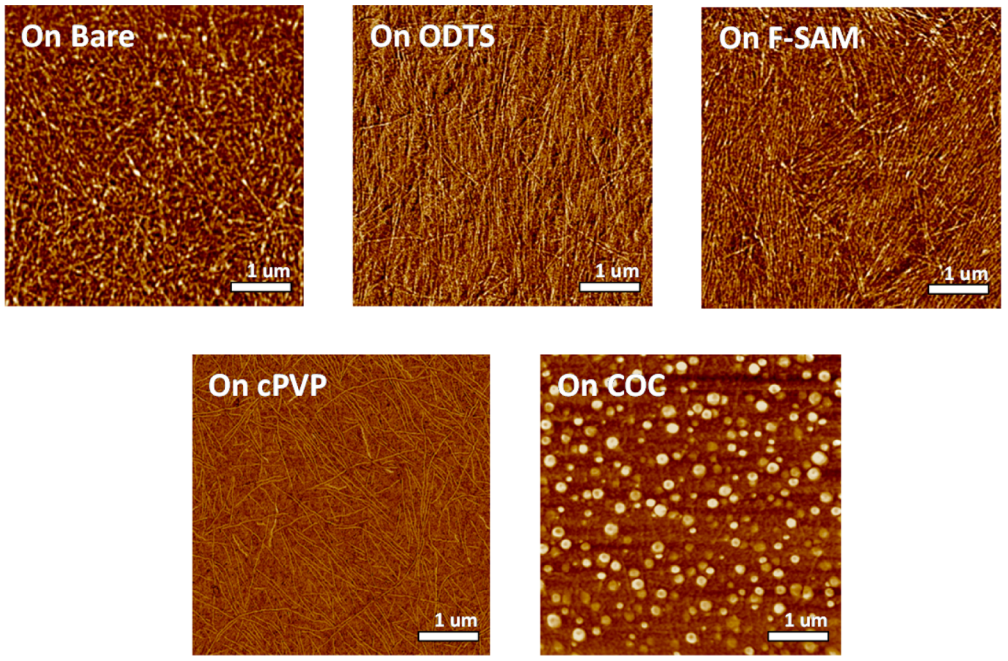

Figure 2. Phase-mode AFM images of an EHD jet printed line of P3HT on bare SiO_2 as well as ODTS-modified, F-SAM-modified, cPVP-treated, and COC-treated substrates.

surface. However, the bulging effect was shown in the optical microscope images of the P3HT lines on the F-SAM surface, as shown in Figure 1d. At low printing speed, a relatively high volume rate could be ejected on the substrate, forming the bulging.[19] To prevent the bulging effect for fine printed lines, further optimization of the printing conditions should be determined in the case of hydrophobic surfaces. The widths of the P3HT lines on polymer thin films, including cPVP and COC, followed similar trends: the width decreased as the surface energy decreased. This result demonstrates that the width of the P3HT line was affected by the surface energy, regardless of the surface modification methods. Supporting Information Figure S1a,b shows the captured optical images of seeding water and P3HT solution drops on the five different types of surface-treated SiO_2/Si substrates with their contact angle values. The water contact angle on F-SAM-modified substrates had the highest value of 107°, followed by ODTS (97°), COC (91°), cPVP (69°), and bare (<1°). In addition, the contact angle of P3HT solution on F-SAM-modified substrates had a value of 65°, followed by ODTS (28°), COC (16°), cPVP (10°), and bare (<3°). Although the contact angle values of P3HT solution on the five different types of surface-treated substrates were different from those of water, their order showed the same tendency as the order of water contact angles and the reverse order of surface energies. We found that as the water and P3HT solution contact angle increased, the printed P3HT line width decreased. When P3HT solution was printed on the bare surface, the solution immediately spread out widely on the bare surface, thereby showing the highest line width. On the other hand, the P3HT solution did not spread widely in the in-plane direction when the solution was dropped on the hydrophobic surfaces. Therefore, we believe that the width of the P3HT line was affected by the surface properties, including the surface energy and wettability of the P3HT solution.

The line morphology was further analyzed using AFM. Figure 2 shows the phase-mode AFM images of printed P3HT on various substrates. After thermal annealing at 150 °C to enhance crystallinity,[30] the P3HT formed distinct nanofibrillar structures with widths of tens of nanometers in scale on SAM- and cPVP-treated surfaces. Actually, spin-coated P3HT thin films on the CH_3-terminated SAM, fluorinated SAM, and cPVP surfaces formed nanofibrillar structures.[26,31,32] On the other hand, the isolated P3HT domains formed when the line was printed on the COC-treated surface. The different morphologies were probably because the COC thin film dewetted the P3HT/toluene solution, disrupting the fibrillar growth of P3HT during solvent evaporation. Figure S2 in the Supporting Information shows the θ-2θ mode out-of-plane XRD patterns of P3HT deposited by spin coating and EHD printing on ODTS-modified substrates, respectively. The diffraction patterns of P3HT consisted of [00l] peaks with the d-spacing obtained from Bragg's law, $2d \sin\theta = n\lambda$, of 16.4 Å for spin coating and 16.0 Å for EHD printing, respectively. These d-values corresponded to the typical edge-on structure in P3HT (16.1 Å),[26] indicating that both the P3HT molecules deposited by spin coating and EHD printing were stacked in the same way in the out-of-plane direction. Though the peak intensity of EHD-printed P3HT is smaller than that of spin-coated P3HT, this is because of the difference in detected P3HT area.

To investigate the effects of the surface modification on the device characteristics of EHD-printed P3HT OFETs, electrical measurements were taken with an OFET structure, as shown in Figure 3a. Au S/D electrodes are deposited on three P3HT lines (four lines in the case of F-SAM) to achieve top-contact OFETs. F-SAM was held with four lines so that both channel widths of ODTS- and F-SAM-OFETs were similar because the width of the printed lines on the F-SAM-modified surface was quite thinner than that on the surface with the other treatments. Figure 3b and S3 show the transfer and output characteristics of P3HT OFETs prepared on the five different types of surface-treated SiO_2/Si substrates, respectively. The length of the channels was 100 μm, and the width of the channels was determined according to the P3HT line width.

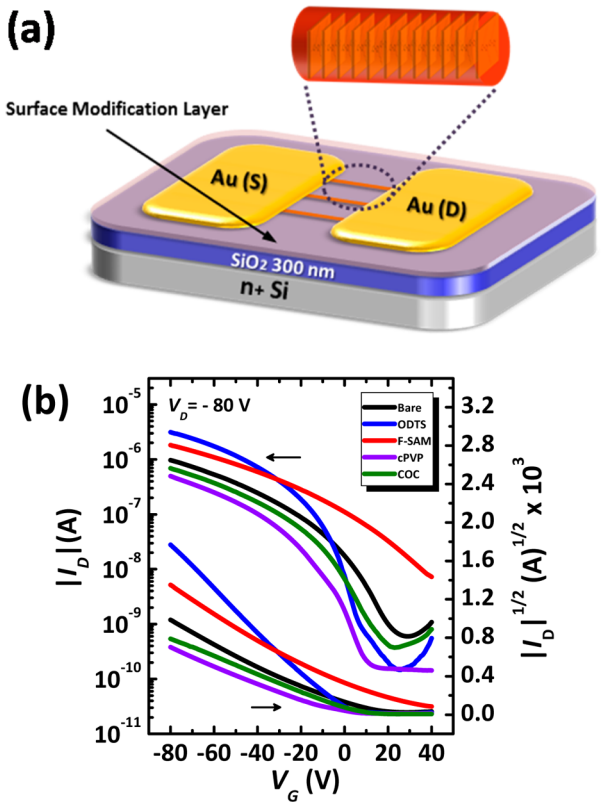

Figure 3. (a) Schematic illustration of EHD-printed P3HT OFETs used in this study. The inset presents an optical microscope image of Au S/D electrodes on the P3HT line. (b) Transfer characteristics in the saturation regime (V_D = −80 V) of nontreated (bare), ODTS-modified, F-SAM-modified, cPVP-treated, and COC-treated OFETs, respectively.

The field-effect mobility (μ) was calculated in the saturation regime (drain voltage, V_D = −80 V) from the slope of the square-root drain current ($I_D^{1/2}$) versus the gate voltage (V_G) using the following equation

$$I_D = \frac{\mu C_i W}{2L}(V_G - V_{th})^2 \quad (2)$$

where C_i is the capacitance per unit area of the gate dielectrics (≈10 nF/cm^2) and V_{th} is the threshold voltage. All of the maximum electrical characteristics of these OFETs are summarized in Table 1, and the detailed electrical characteristics, including the channel length, mobility, and on-currents, of these three different OFETs are summarized in Supporting Information Table S1. Compared to the OFETs without surface treatment (i.e., bare SiO_2), the SAM-modified OFETs showed higher mobility and on-state currents. Among these OFETs, the ODTS-modified devices exhibited the highest transistor performance, with a μ value of 0.045 cm^2/(V s) and a high on/off ratio of 2.1 × 10^4, comparable to that of other reported P3HT OFETs on an oxide dielectric layer prepared with inkjet printing, spray printing, or electrospinning methods.[6,7,21,30,33−35] For OFETs with F-SAM modification, the V_{th} value shifts to a positive voltage because of the generation of the local built-in electric field that accumulates holes on the interface between the P3HT and F-SAM-modified dielectric surface.[36] Moreover, F-SAM OFETs yield the lowest on/off ratio, with a high off-current value of over 10^{-8} A because the accumulated holes provided a current pathway even in the off-state. Therefore, EHD-printed P3HT OFETs with F-SAM modification showed typical normally on-type characteristics, such as that of spin-coated P3HT OFETs.[37] A normally on-type characteristic means that electric current flows without gate bias voltage.[32,36,38] Therefore, the normally on-type devices showed a high off-current and small on/off ratio. On the other hand, the transistor performances of OFETs with polymer treatments were almost the same as those of the OFETs without surface treatment. The only difference between cPVP-treated and bare OFETs was V_{th}, in which the cPVP-treated OFETs had a lower value than that of the bare OFETs. Although PVP is known as a hydroxyl-rich polymer, the cross-linking reaction with an adequate amount of PMF reduces the number of hydroxyl groups on SiO_2, contributing to the blocking of hole trap formation.[28] The OFETs on the COC-treated surface showed a higher off-current than those on the cPVP-treated surface. Because the isolated and rough P3HT domain morphology on COC-treated surface was vulnerable to penetration of H_2O and O_2 into the bulk region when exposed to air during EHD printing, the P3HT on COC-treated surface was easily doped by penetrated H_2O and O_2, thereby increasing the off-current.[6,39,40] Therefore, we believe that the electrical performances of EHD-printed P3HT OFETs were affected by the type of surface-modifying materials coated on the dielectric layers.

Table 1. Electrical Characteristics of EHD Jet Printed P3HT OFETs with Various Surface Treatments

gate dielectric surface	mobility μ (cm^2/(V s))	threshold voltage V_{th} (V)	on/off ratio (I_{ON}/I_{OFF})
bare	0.008	−3.47	1.6 × 10^3
ODTS	0.045	−3.35	2.1 × 10^4
F-SAM	0.021	9.51	2.2 × 10^2
cPVP	0.007	−2.70	3.2 × 10^4
COC	0.008	−3.97	1.8 × 10^3

Because these results were obtained without characterizing the proper solvent and annealing conditions for P3HT, the electrical performance of EHD-printed P3HT OFETs has the potential to be enhanced with additional effort.

For practical applications, we attempted to fabricate a large-area device array including 100 bottom-contact (BC) OFETs on a 4 in. wafer, as shown in Figure 4a. The BC device configuration is required to avoid the possible damage of organic semiconductor layers deposited after patterning the S/D electrodes.[41,42] For the fabrication, the 4 in. wafer was modified with ODTS in the same way as that of the top-contact single device, and the P3HT lines were also successfully printed on the predeposited Au S/D with different line widths. It took only 10 s to print a single line on the wafer. Figure 4b shows the transfer characteristic for one BC OFET of the device array. The average μ value was 0.023 ± 0.008 cm^2/(V s), which was lower than that of the top-contact devices because of the poor contact characteristic between the P3HT active layers and the S/D electrodes.[41]

We then printed P3HT on flexible PES substrates to achieve flexible, low-operating-voltage OFETs. For the fabrication, aluminum was deposited on PES substrates as a gate electrode, and then an amorphous alumina (Al_2O_3) dielectric layer with high C_i (≈140 nF/cm^2) was deposited by PEALD, followed by ODTS surface modification. ODTS-modified Al_2O_3 gate dielectrics are known to facilitate low-voltage, high-performance operation of the OFETs because of the high capacitance and

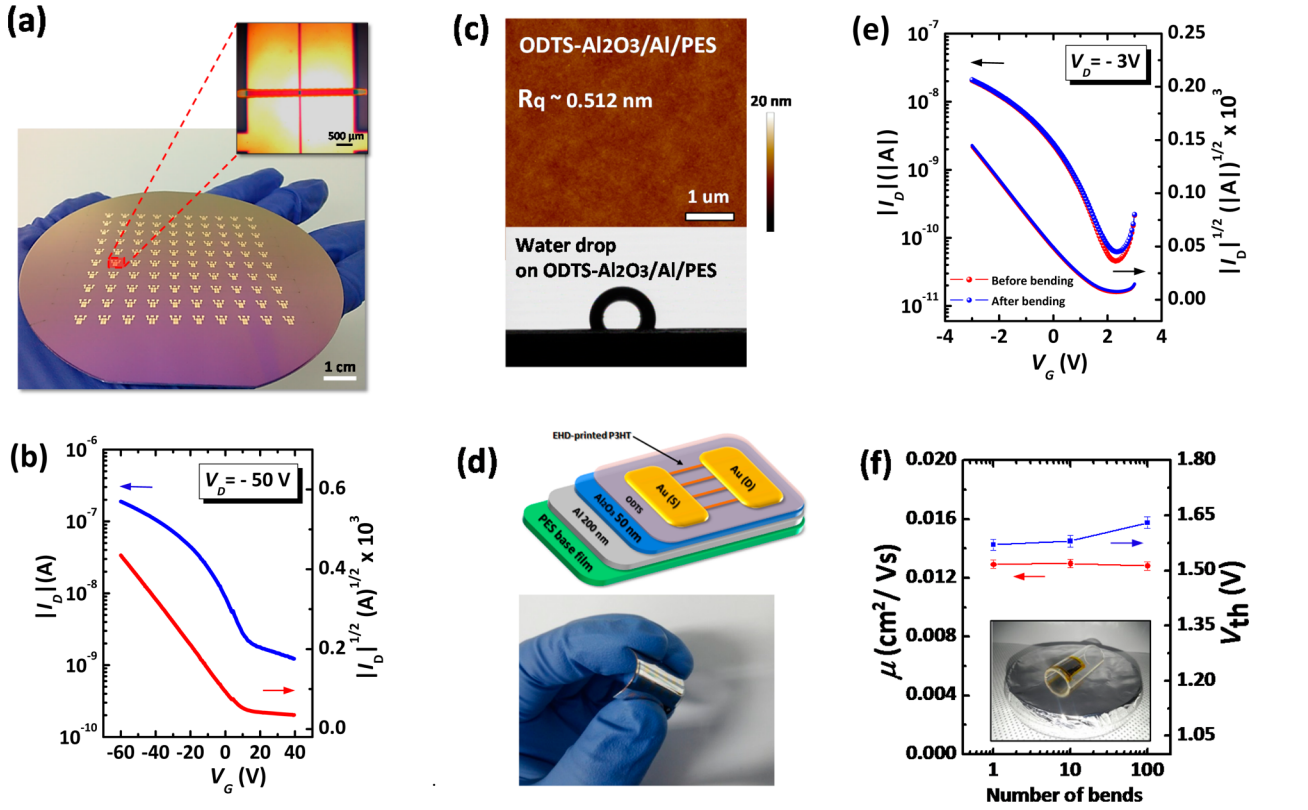

Figure 4. (a) Captured digital image of large-area transistor array including 100 EHD-printed P3HT OFETs. The inset image represents an optical microscope image of the P3HT line on Au S/D electrodes and channel. (b) Transfer characteristics in the saturation regime (V_D = −50 V) of one BC OFET of the 100 BC device. (c) Height-mode AFM images of ODTS-treated Al_2O_3 dielectric surfaces (top) as well as a captured optical image of seeding water drops on the ODTS-treated dielectric surface (bottom). (d) Schematic illustration of an EHD-printed P3HT OFETs employing Al_2O_3 dielectrics and PES substrates (top) as well as a captured bending image of flexible OFETs (bottom). (e) Transfer characteristics (V_D = −3 V) of the flexible OFETs. (f) μ and V_{th} versus number of bending cycles. The inset presents an image of an OFET bent over a 0.5 cm radius.

low trap density.[43] The height-mode AFM image, as shown in Figure 4c, revealed that the ODTS-modified Al_2O_3/Al/PES device surfaces were very smooth, with an rms roughness (R_q) of 0.512 nm within the 5 × 5 μm^2 scan. The value of the water contact angle (θ_{water}) was measured to confirm that the substrate was effectively modified with ODTS. The value of θ_{water} derived from the captured images of water drops (Figure 4c) was 98°, which is similar to the θ_{water} value on ODTS-modified SiO_2/Si. These results suggest that the surface of Al_2O_3/Al/PES was successfully modified with ODTS. The full device structure, transfer characteristics, and device-bending stress tests are summarized in Figure 4d−f. This flexible OFET exhibited typical low-operating-voltage *p*-type transfer characteristics within the operating voltages from 3 to −3 V. The average μ and V_{th} values are 0.013 ± 0.007 $cm^2/(V\,s)$ and 1.57 V, respectively. For the bending experiments, the flexible OFETs were bent with a bending radius (R) of 0.5 cm, constituting a bending strain (ε) of 1.5% on the devices, as calculated using the equation $\varepsilon = D/2R$, where D is sample thickness (D = 150 μm).[14,44,45] From the bending tests, we found that these devices sustained electrical performances after 100 repeated bends: μ and V_{th} changed by ∼5%. These results demonstrate that the EHD printing approach is a promising technology for large-area flexible devices.

CONCLUSIONS

We developed a direct writing approach from EHD jet printing as a simple line-patterning method for P3HT and demonstrated the potential application of this method for the fabrication of large area, flexible, and low--operating-voltage organic transistors. A straight line with microscale dimensions was stably obtained by applying electric fields. We investigated the effect of the surface energy and type of substrate on the line width, P3HT morphology, and OFET performance. We found that OFETs from EHD jet printed P3HT on the ODTS-modified surface exhibited good electrical performances comparable to those using other printing methods. We believe that EHD printing technology will contribute to the realization of low-cost, large-area printed organic integrated devices.

ASSOCIATED CONTENT

Supporting Information

Captured optical images of seeding water drops and P3HT solution drops on the five different types of surface treated SiO_2/Si substrates with their contact angle values; θ–2θ mode out-of-plane XRD profiles of the P3HT deposited by spin coating and EHD printing; output characteristics of nontreated, ODTS-modified, F-SAM-modified, c-PVP-treated, and COC-treated OFETs; and comparison of the channel widths and electrical characteristics of EHD jet printed OFETs with various surface treatments. This material is available free of charge via the Internet at http://pubs.acs.org.

AUTHOR INFORMATION

Corresponding Authors

*(J.-J.P.) E-mail: jongjin00.park@samsung.com; Tel: +82-31-280-6728.

*(C.E.P.) E-mail: cep@postech.ac.kr; Fax: +82-54-279-8298; Tel: +82-54-279-2269.

*(D.B.) E-mail: dybyun@skku.edu; Tel: +82-31-299-4846.

Author Contributions

‖Y.J.J. and H.L. contributed equally to this work.

Notes

The authors declare no competing financial interest.

ACKNOWLEDGMENTS

This research was supported by the Basic Science Research Program through the National Research Foundation of Korea (NRF), funded by the Ministry of Education, Science and Technology (MEST, 2011-0016461). This work was also supported by a grant from the National Research Foundation of Korea (NRF), funded by the Korean Government (MSIP) (2014R1A2A1A05004993). The authors thank the Pohang Accelerator Laboratory for providing access to the 5A beamlines used in this study.

REFERENCES

(1) Forrest, S. R. The Path to Ubiquitous and Low-Cost Organic Electronic Appliances on Plastic. *Nature* **2004**, *428*, 911−918.

(2) Baude, P. F.; Ender, D. A.; Haase, M. A.; Kelley, T. W.; Muyres, D. V.; Theiss, S. D. Pentacene-Based Radio-Frequency Identification Circuitry. *Appl. Phys. Lett.* **2003**, *82*, 3964.

(3) Someya, T.; Sekitani, T.; Iba, S.; Kato, Y.; Kawaguchi, H.; Sakurai, T. A Large-Area, Flexible Pressure Sensor Matrix with Organic Field-Effect Transistors for Artificial Skin Applications. *Proc. Natl. Acad. Sci. U.S.A.* **2004**, *101*, 9966−9970.

(4) Kaltenbrunner, M.; Sekitani, T.; Reeder, J.; Yokota, T.; Kuribara, K.; Tokuhara, T.; Drack, M.; Schwödiauer, R.; Graz, I.; Bauer-Gogonea, S.; Bauer, S.; Someya, T. An Ultra-Lightweight Design for Imperceptible Plastic Electronics. *Nature* **2013**, *499*, 458−463.

(5) Kim, J.-M.; Jha, S. K.; Lee, D.-H.; Chand, R.; Jeun, J.-H.; Kim, Y.-S. A Flexible Pentacene Thin Film Transistors as Disposable DNA Hybridization Sensor. *J. Ind. Eng. Chem.* **2012**, *18*, 1642−1646.

(6) Lim, J. A.; Kim, J.-H.; Qiu, L.; Lee, W. H.; Lee, H. S.; Kwak, D.; Cho, K. Inkjet-Printed Single-Droplet Organic Transistors Based on Semiconductor Nanowires Embedded in Insulating Polymers. *Adv. Funct. Mater.* **2010**, *20*, 3292−3297.

(7) Chan, C. K.; Richter, L. J.; Dinardo, B.; Jaye, C.; Conrad, B. R.; Ro, H. W.; Germack, D. S.; Fischer, D. A.; DeLongchamp, D. M.; Gundlach, D. J. High Performance Airbrushed Organic Thin Film Transistors. *Appl. Phys. Lett.* **2010**, *96*, 133304.

(8) Sirringhaus, H. High-Resolution Inkjet Printing of All-Polymer Transistor Circuits. *Science* **2000**, *290*, 2123−2126.

(9) Russo, A.; Ahn, B. Y.; Adams, J. J.; Duoss, E. B.; Bernhard, J. T.; Lewis, J. A. Pen-on-Paper Flexible Electronics. *Adv. Mater.* **2011**, *23*, 3426−3430.

(10) Kang, B.; Min, H.; Seo, U.; Lee, J.; Park, N.; Cho, K.; Lee, H. S. Directly Drawn Organic Transistors by Capillary Pen: A New Facile Patterning Method Using Capillary Action for Soluble Organic Materials. *Adv. Mater.* **2013**, *25*, 4117−4122.

(11) Nam, S.; Jeon, H.; Kim, S.; Jang, J.; Yang, C.; Park, C. An Inkjet-Printed Passivation Layer Based on a Photocrosslinkable Polymer for Long-Term Stable Pentacene Field-Effect Transistors. *Org. Electron.* **2009**, *10*, 67−72.

(12) Saito, Y.; Sakai, Y.; Higashihara, T.; Ueda, M. Direct Patterning of Poly(3-hexylthiophene) and Its Application to Organic Field-Effect Transistor. *RSC Adv.* **2012**, *2*, 1285.

(13) Choi, J.; Kim, Y.-J.; Lee, S.; Son, S. U.; Ko, H. S.; Nguyen, V. D.; Byun, D. Drop-on-Demand Printing of Conductive Ink by Electrostatic Field Induced Inkjet Head. *Appl. Phys. Lett.* **2008**, *93*, 193508.

(14) Kim, S. H.; Hong, K.; Lee, K. H.; Frisbie, C. D. Performance and Stability of Aerosol-Jet-Printed Electrolyte-Gated Transistors Based on Poly(3-hexylthiophene). *ACS Appl. Mater. Interfaces.* **2013**, *5*, 6580−6585.

(15) Sun, D.; Chang, C.; Li, S.; Lin, L. Near-Field Electrospinning. *Nano Lett.* **2006**, *6*, 839−842.

(16) Zheng, G.; Li, W.; Wang, X.; Wu, D.; Sun, D.; Lin, L. Precision Deposition of a Nanofibre by Near-Field Electrospinning. *J. Phys. D: Appl. Phys.* **2010**, *43*, 415501.

(17) Duan, Y.; Huang, Y.; Yin, Z.; Bu, N.; Dong, W. Non-wrinkled, Highly Stretchable Piezoelectric Devices by Electrohydrodynamic Direct-Writing. *Nanoscale* **2014**, *6*, 3289−3295.

(18) Huang, Y.; Wang, X.; Duan, Y.; Bu, N.; Yin, Z. Controllable Self-organization of Colloid Microarrays Based on Finite Length Effects of Electrospun Ribbons. *Soft Matter* **2012**, *8*, 8302.

(19) Jang, Y.; Hartarto Tambunan, I.; Tak, H.; Dat Nguyen, V.; Kang, T.; Byun, D. Non-contact Printing of High Aspect Ratio Ag Electrodes for Polycrystalline Silicone Solar Cell with Electrohydrodynamic Jet Printing. *Appl. Phys. Lett.* **2013**, *102*, 123901.

(20) Jang, Y.; Kim, J.; Byun, D. Invisible Metal-Grid Transparent Electrode Prepared by Electrohydrodynamic (EHD) Jet Printing. *J. Phys. D: Appl. Phys.* **2013**, *46*, 155103.

(21) Min, S. Y.; Kim, T. S.; Kim, B. J.; Cho, H.; Noh, Y. Y.; Yang, H.; Cho, J. H.; Lee, T. W. Large-Scale Organic Nanowire Lithography and Electronics. *Nat. Commun.* **2013**, *4*, 1773.

(22) Lee, S.; Byun, D.; Jung, D.; Choi, J.; Kim, Y.; Yang, J. H.; Son, S. U.; Tran, S. B. Q.; Ko, H. S. Pole-Type Ground Electrode in Nozzle for Electrostatic Field Induced Drop-on-Demand Inkjet Head. *Sens. Actuators, A* **2008**, *141*, 506−514.

(23) Nguyen, V. D.; Byun, D. Mechanism of Electrohydrodynamic Printing Based on ac Voltage without a Nozzle Electrode. *Appl. Phys. Lett.* **2009**, *94*, 173509.

(24) Kim, D. H.; Jang, Y.; Park, Y. D.; Cho, K. Layered Molecular Ordering of Self-organized Poly(3-hexylthiophene) Thin Films on Hydrophobized Surfaces. *Macromolecules* **2006**, *39*, 5843−5847.

(25) Kinloch, A. J. *Adhesion and Adhesives: Science and Technology*; Chapman and Hall: London, 1987; pp 18−32.

(26) Choi, D.; An, T. K.; Kim, Y. J.; Chung, D. S.; Kim, S. H.; Park, C. E. Effects of Semiconductor/Dielectric Interfacial Properties on the Electrical Performance of Top-Gate Organic Transistors. *Org. Electron.* **2014**, *15*, 1299−1305.

(27) Jang, J.; Nam, S.; Chung, D. S.; Kim, S. H.; Yun, W. M.; Park, C. E. High Tg Cyclic Olefin Copolymer Gate Dielectrics for N,N′-Ditridecyl Perylene Diimide Based Field-Effect Transistors: Improving Performance and Stability with Thermal Treatment. *Adv. Funct. Mater.* **2010**, *20*, 2611−2618.

(28) Kim, S. H.; Nam, S.; Jang, J.; Hong, K.; Yang, C.; Chung, D. S.; Park, C. E.; Choi, W.-S. Effect of The Hydrophobicity and Thickness of Polymer Gate Dielectrics on The Hysteresis Behavior of Pentacene-based Field-effect Transistors. *J. Appl. Phys.* **2009**, *105*, 104509.

(29) Prasetyo, F. D.; Yudistira, H. T.; Nguyen, V. D.; Byun, D. Ag Dot Morphologies Printed Using Electrohydrodynamic (EHD) Jet Printing Based on a Drop-on-Demand (DOD) Operation. *J. Micromech. Microeng.* **2013**, *23*, 095028.

(30) Chen, J.-Y.; Kuo, C.-C.; Lai, C.-S.; Chen, W.-C.; Chen, H.-L. Manipulation on the Morphology and Electrical Properties of Aligned Electrospun Nanofibers of Poly(3-hexylthiophene) for Field-Effect Transistor Applications. *Macromolecules* **2011**, *44*, 2883−2892.

(31) Sethuraman, K.; Ochiai, S.; Kojima, K.; Mizutani, T. Performance of Poly(3-hexylthiophene) Organic Field-Effect Transistors on Cross-Linked Poly(4-vinyl phenol) Dielectric Layer and Solvent Effects. *Appl. Phys. Lett.* **2008**, *92*, 183302.

(32) Karakawa, M.; Chikamatsu, M.; Yoshida, Y.; Oishi, M.; Azumi, R.; Yase, K. High-Performance Poly(3-hexylthiophene) Field-Effect Transistors Fabricated by a Slide-Coating Method. *Appl. Phys. Express* **2008**, *1*, 061802.

(33) Po-Yuan, L.; Pei-Wen, L.; Zing-Way, P.; Hou, J.; Chan, Y.-J. Enhanced P3HT OTFT Transport Performance Using Double Gate Modulation Scheme. *IEEE Electron Device Lett.* **2009**, *30*, 629−631.
(34) Liu, H.; Reccius, C. H.; Craighead, H. G. Single Electrospun Regioregular Poly(3-hexylthiophene) Nanofiber Field-Effect Transistor. *Appl. Phys. Lett.* **2005**, *87*, 253106.
(35) Lee, S.; Moon, G. D.; Jeong, U. Continuous Production of Uniform Poly(3-hexylthiophene) (P3HT) Nanofibers by Electrospinning and Their Electrical Properties. *J. Mater. Chem.* **2009**, *19*, 743.
(36) Kobayashi, S.; Nishikawa, T.; Takenobu, T.; Mori, S.; Shimoda, T.; Mitani, T.; Shimotani, H.; Yoshimoto, N.; Ogawa, S.; Iwasa, Y. Control of Carrier Density by Self-assembled Monolayers in Organic Field-Effect Transistors. *Nat. Mater.* **2004**, *3*, 317−322.
(37) Horii, Y.; Ikawa, M.; Sakaguchi, K.; Chikamatsu, M.; Yoshida, Y.; Azumi, R.; Mogi, H.; Kitagawa, M.; Konishi, H.; Yase, K. Investigation of Self-assembled Monolayer Treatment on SiO_2 Gate Insulator of Poly(3-hexylthiophene) Thin-Film Transistors. *Thin Solid Films* **2009**, *518*, 642−646.
(38) Pernstich, K. P.; Goldmann, C.; Krellner, C.; Oberhoff, D.; Gundlach, D. J.; Batlogg, B. Shifted Transfer Characteristics of Organic Thin Film and Single Crystal FETs. *Synth. Met.* **2004**, *146*, 325−328.
(39) Qiu, Y.; Hu, Y.; Dong, G.; Wang, L.; Xie, J.; Ma, Y. H_2O Effect on The Stability of Organic Thin-Film Field-Effect Transistors. *Appl. Phys. Lett.* **2003**, *83*, 1644.
(40) Majewski, L. A.; Kingsley, J. W.; Balocco, C.; Song, A. M. Influence of Processing Conditions on the Stability of Poly(3-hexylthiophene)-Based Field-Effect Transistors. *Appl. Phys. Lett.* **2006**, *88*, 222108.
(41) Hong, Y.; Yan, F.; Migliorato, P.; Han, S. H.; Jang, J. Injection-Limited Contact in Bottom-Contact Pentacene Organic Thin-Film Transistors. *Thin Solid Films* **2007**, *515*, 4032−4035.
(42) Hong, K.; Kim, S. H.; Yang, C.; Jang, J.; Cha, H.; Park, C. E. Improved n-Type Bottom-Contact Organic Transistors by Introducing a Poly(3,4-ethylenedioxythiophene):Poly(4-styrene sulfonate) Coating on the Source/Drain Electrodes. *Appl. Phys. Lett.* **2010**, *97*, 103304.
(43) Nam, S.; Jang, J.; Park, J.-J.; Kim, S. W.; Park, C. E.; Kim, J. M. High-Performance Low-Voltage Organic Field-Effect Transistors Prepared on Electro-Polished Aluminum Wires. *ACS Appl. Mater. Interfaces.* **2012**, *4*, 6−10.
(44) Yang, C.; Yoon, J.; Kim, S. H.; Hong, K.; Chung, D. S.; Heo, K.; Park, C. E.; Ree, M. Bending-Stress-Driven Phase Transitions in Pentacene Thin Films for Flexible Organic Field-Effect Transistors. *Appl. Phys. Lett.* **2008**, *92*, 243305.
(45) Sekitani, T.; Kato, Y.; Iba, S.; Shinaoka, H.; Someya, T.; Sakurai, T.; Takagi, S. Bending Experiment on Pentacene Field-Effect Transistors on Plastic Films. *Appl. Phys. Lett.* **2005**, *86*, 073511.